Available online at www.sciencedirect.com
SCIENCE DIRECT®
Journal of Crystal Growth 253 (2003) 221–229
JOURNAL OF CRYSTAL GROWTH
www.elsevier.com/locate/jcrysgro

Growth and characterization of 3-in size Tm, Ho-codoped $LiYF_4$ and $LiLuF_4$ single crystals by the Czochralski method

Hiroki Sato[a,b,*], Amina Bensalah[a], Hiroshi Machida[b], Martin Nikl[c], Tsuguo Fukuda[a]

[a] *Institute of Multidisciplinary Research for Advanced Materials, Tohoku University, 2-1-1 Katahira, Aoba-ku, Sendai 980-8577 Japan*
[b] *NEC TOKIN Corporation, 28-1 Hanashimashinden, Tsukuba, Ibaraki 305-0875 Japan*
[c] *Institute of Physics ASCR, Cukrovarnicka 10, 16253 Prague, Czech Republic*

Received 20 January 2003; accepted 2 February 2003
Communicated by M. Schieber

Abstract

Tm, Ho-codoped $LiYF_4$ (Tm,Ho:YLF) and Tm, Ho-codoped $LiLuF_4$ (Tm,Ho:LLF) single crystals with extended diameter were grown by the Czochralski method under CF_4 atmosphere. The growth conditions were optimized for the growth of Tm,Ho:YLF and Tm,Ho:LLF single crystals with 3-in diameters. The crystallinity was studied using X-ray rocking curve analysis. Color center formation in the ultraviolet and visible spectral regions was investigated with the induced absorption study using X-ray irradiation.

PACS: 42.88.+h; 76.30.Mi; 78.40.Ha; 78.20.Ci; 81.10.Fq

Keywords: A1. Induced absorption; A2. Crystal growth from melt; A2. Czochralski method; B1. $LiYF_4$; B1. $LiLuF_4$; B3. Eye-safe laser

1. Introduction

During the last few years, interest in high-energy laser operating in the 2 μm spectral region has increased because of the availability of high power quasi-CW laser diode arrays (LDAs), and introduction of a variety of applications that require eye-safe lasers that propagate through the atmosphere. Two micron laser sources are potentially useful for a variety of applications, including coherent Doppler velocimetry, gas detection [1] and space applications such as atmospheric wind sensors for full-scale earth observation satellites. Moreover, there are also medical applications since liquid water has strong absorption in this wavelength region [2,3].

Two micron lasers based on Tm $^3F_4$–$^3H_6$ and Tm $^3H_4$–$^3H_5$ transitions have been reported in

*Corresponding author. Institute of Multidisciplinary Research for Advanced Materials, Tohoku University, 2-1-1 Katahira, Aoba-ku, Sendai 980-8577 Japan. Tel.: +81-22-217-5167; fax: +81-22-217-5102.
E-mail address: sato-h@mail.tagen.tohoku.ac.jp (H. Sato).

0022-0248/03/$ - see front matter
doi:10.1016/S0022-0248(03)00998-9

several crystalline materials [1,4]. Ho $^5I_7$–$^5I_8$ transition has a markedly higher lasing emission cross section than the Tm $^3F_4$–$^3H_6$ transition [5]. However, Ho does not have an absorption band to match the emission of commercially available laser diodes and hence there is a need for co-doping with thulium. Room temperature laser emission at 2 μm based on holmium (Ho) $^5I_7$–$^5I_8$ transition is reported in several Tm, Ho-codoped garnets [6–11]. However, Tm, Ho-codoped oxide crystals show more severe up-conversion losses compared to Tm, Ho-codoped fluorides. We therefore, investigated Tm, Ho-codoped $LiYF_4$ (Tm,Ho:YLF) and Tm, Ho-codoped $LiLuF_4$ (Tm,Ho:LLF) laser crystals.

YLF and LLF both crystallize in a scheelite structure (tetragonal system and I41/a space group). Growth and characterization of Tm,Ho:YLF have previously been reported [12–15]. In contrast, only a few studies on Tm,Ho:LLF have been done, mainly because good quality LLF crystals are difficult to grow [16]. As indicated before, the growth of optically clear fluoride single crystals depends not only on the growth process itself, but also on the purity of the starting materials and the presence of oxygen-containing complexes in the environment [17–19]. We previously reported the growth and characterization of 1-in in size Tm,Ho:YLF and Tm,Ho:LLF single crystals without either the use of HF gases or the hydrofluorination of raw materials [20].

In the present work, we describe the growth of Tm,Ho:YLF and LLF single crystals with extended diameters by the Czochralski (Cz) technique under modified growth conditions based on the investigations reported in Refs. [17–19]. Fundamental properties of Tm,Ho:YLF and Tm,Ho:LLF single crystals such as the variations in the lattice parameter and thermal expansion coefficient have been addressed. Another aim of this paper is to provide a systematic overlook of X-ray induced color centers and trapping phenomena in Tm,Ho:YLF and Tm,Ho:LLF single crystals. We describe X-ray induced radiation damage using optical absorption measurements in the ultra violet (UV), visible (VIS) and infrared (IR) spectra regions.

2. Experimental procedure

Crystal growth was performed in a Cz system with a resistive heater made of high-purity graphite. The starting material was prepared from commercially available LiF, YF_3 and LuF_3 powders of high purity (>99.99%). As dopants, TmF_3 and HoF_3 powders of high purity (>99.99%) were used. The concentrations of Tm and Ho in the starting material were 5 and 0.5 mol%, respectively. The starting material was placed in a Pt crucible. Vacuum treatment was performed prior to growth. The system was heated from room temperature to 700°C for a period of 12 h under vacuum ($\approx 10^{-3}$ Pa). Both rotary and diffusion pumps were used to achieve $\approx 10^{-3}$ Pa and effectively eliminate water and oxygen from the growth chamber and the starting material. Subsequently, high-purity CF_4 gas (99.99%) was slowly introduced into the furnace. Thereafter, the starting materials were melted at approximately 860°C. After growth, the crystals were cooled down to room temperature at a rate of 20°C/h.

Powder X-ray diffraction (XRD) measurements for lattice parameter determination were carried out on a Rigaku diffractometer (RIGAKU RINT 2000), operated at 40 kV and 40 mA in the 2θ range of 5–30° using MoKα X-ray source. The dependence of the lattice parameter on temperature was measured using a high temperature XRD method under high-purity nitrogen (99.999%) gas flow atmosphere. The scan rate was 10°C/min. In order to stabilize the temperature of the samples at each temperature, a wait period of 10 min was given before starting the XRD scan which took 90 min for each temperature. The thermal expansion coefficients were determined by the thermomechanical analyzing using A TMA 8310 apparatus. Specimens for this measurement were prepared in a rectangular parallelepiped shape from the Tm,Ho:YLF and Tm,Ho:LLF crystals, and had dimensions of $4 \times 4 \times 15\,mm^3$, with *a*- or *c*-axis in the longitudinal direction, respectively.

The crystal quality of the Tm,Ho:YLF and Tm,Ho:LLF single crystals, corresponding to the width of the peak, was characterized by X-ray rocking curve (XRC) measurement using RIGAKU ATX-E with a 4-bounce Ge (2 2 0) channel-cut

monochromator. In order to obtain correct FWHM values from ω scan profile measurements, appropriate X-ray optics with respect to the sample quality is necessary. In our setup the beam divergence was 0.003°. A CuKα_1 X-ray source ($\lambda = 1.54056$ Å) was used. Under these conditions, ω scans were carried out.

To test material stability, the Tm,Ho:YLF and Tm,Ho:LLF crystals were irradiated by X-rays. Radiation damage (creating color centers) has been characterized here by the RT measurement of the radiation induced optical absorption. The transmission spectrum was measured by a Jasco V-530 UV/VIS/IR spectrophotometer in the spectral region from 190 to 2000 nm and the induced absorption ($\mu(\lambda)$) was calculated using the following equation:

$$\mu(\lambda) = \ln(T_0(\lambda)/T_{\mathrm{irr}}(\lambda)), \quad (1)$$

where T_0 and T_{irr} are the transmission before and after X-ray irradiation, respectively. It should be taken into account that the samples have high absorption coefficient against X-ray. It is typically achieved in YLF and LLF below 1 mm thickness using standard attenuation calculation according to Ref. [21]. In order to compare, all the samples were prepared with the same thickness of about 2 mm. Irradiation was accomplished by an X-ray tube (25 kV, Rigaku diffractometer). In the case of the induced absorption measurements subsequent irradiation doses were set at 240 Gy.

3. Results and discussion

The growth of Tm,Ho:YLF single crystals with a 2–3-in diameter was investigated. Mixed powder of raw materials was placed in a 100–130 mm diameter Pt crucible. Crystals were grown at a pulling and rotation speed of 1.0 mm/h and 12 rpm, respectively. Fig. 1 shows a 2-in diameter Tm,Ho:YLF crystal with inclusions. Although the diameter of the grown crystal was controlled precisely, a formation of inclusions could not be avoided. Fig. 2 shows a result of XRD measurement of these inclusions. As can be seen, the impurity phase of YF_3 was observed. As the YLF compound melts slightly incongruently and a few LiF evaporate during Tm,Ho:YLF growth process, the starting material was $LiF:YF_3 = 0.52:0.48$, same as 1-in crystal growth [20]. But in the case of 2–3-in size Tm,Ho:YLF crystal growth, the preparation of the starting melt composition in LiF enriched directions was not sufficient. As the vaporization from the melt was thought to be increased because of the extended melt surface area, the starting melt composition had to be prepared in more LiF enriched directions ($LiF:YF_3 = 0.53:0.47$).

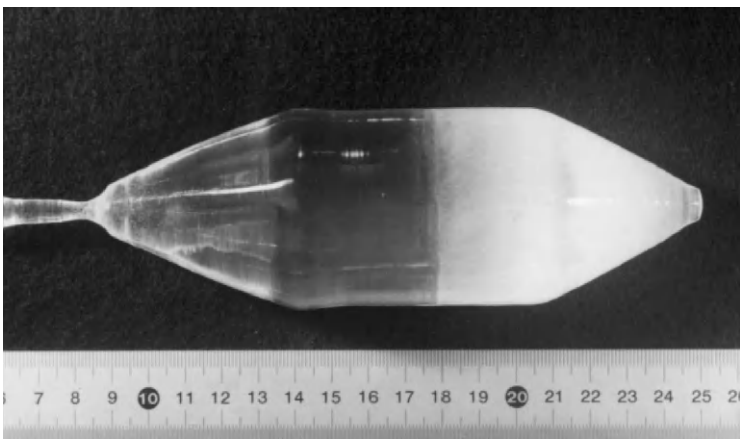

Fig. 1. As-grown 5% Tm and 0.5% Ho-codoped $LiYF_4$ crystal 2 in in diameter with inclusions. There are visible inclusions at the bottom.

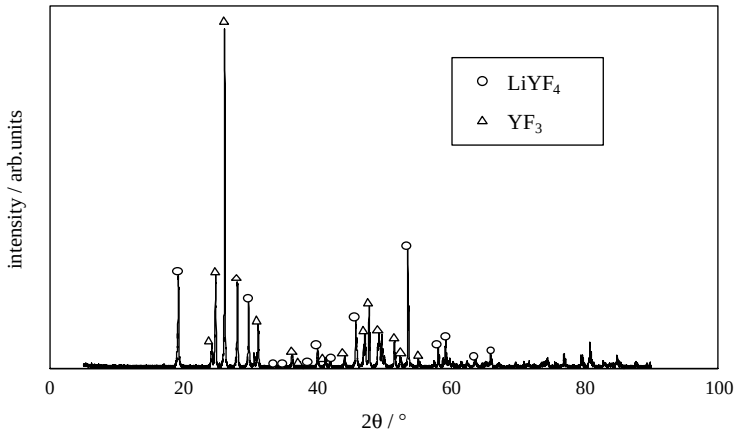

Fig. 2. XRD profile for the inclusions occurred in 2-in size 5% Tm and 0.5% Ho-codoped $LiYF_4$ crystal.

Fig. 3. As-grown 5% Tm and 0.5% Ho-codoped $LiYF_4$ crystal 3 in in diameter with cracks.

Fig. 3 shows a Tm,Ho:YLF crystal grown from the modified chemical composition. The formation of inclusions was not observed, while many cracks appeared in a grown crystal. We understand that this is due to a thermal stress in the grown crystal, since the grown crystal was located at a position where the temperature gradient was high during the cooling process. Especially, more cracks were observed at the shoulder part of the grown crystal. This is because the temperature gradient of the upper part was larger. In the case of crystals grown with a fixed crucible position, the formation of cracks was not observed. When the crucible was not raised, the distance to be pulled up could not be relatively large, because crystals were grown toward the crucible bottom with the distance corresponding to the descent of the melt level. Therefore, grown crystals could not be pulled up to the position where temperature gradient was large. Based on this consideration, the grown crystal and the crucible were lowered to their positions after the crystal growth process, and the grown crystal was cooled at the position where temperature gradient was lower, in order to avoid

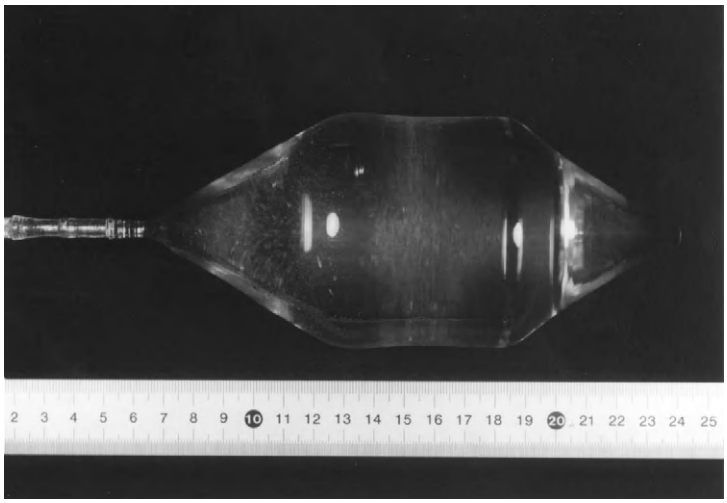

Fig. 4. As-grown 5% Tm and 0.5% Ho-codoped $LiYF_4$ single crystal 3 in in diameter, free from inclusions and cracks.

the formation cracks. Fig. 4 shows a Tm,Ho:YLF single crystal with a 3-in diameter, free from cracks and inclusions.

Fig. 5 shows the XRD profile measured for Tm,Ho:YLF and Tm,Ho:LLF single crystals at different temperatures. From room temperature to 400°C there is no phase change, and both crystals show a single phase. But from 700°C in Tm,Ho:YLF and from 600°C in Tm,Ho:LLF, the different phases such as Li_2O, Y_2O_3 and Lu_2O_3 appeared. As this might be because fluoride powders are easy to oxidize, the measured crystal powders were partially oxidized in spite of using high-purity N_2 gas in the high temperature XRD measurement. Fig. 6 shows the temperature dependence of the lattice parameters. The lattice parameters increase linearly with temperature. Based on the result of Fig. 6, the linear thermal expansion coefficient of Tm,Ho:YLF and Tm,Ho:LLF single crystals were calculated (Table 1).

Fig. 7 shows the thermal expansion along *a*-axis and *c*-axis for Tm,Ho:YLF and Tm,Ho:LLF crystals. From this figure, the thermal expansion coefficients of Tm,Ho:YLF and Tm,Ho:LLF were estimated over the range of 30–500°C and these values are given in Table 1. The linear thermal expansion coefficient calculated from the lattice parameters of the XRD measurement and the thermal expansion coefficient should have the same value. Table 1 shows each value is almost the same.

The crystal quality of the grown crystal was characterized by XRC measurements. ω scan was carried out for the reflection from (400) plane corresponding to the $<100>$ direction. The spectra for Tm,Ho:YLF and Tm,Ho:LLF crystals are shown in Fig. 8. It is shown that the FWHMs for Tm,YLF and Tm,Ho:LLF were measured to be 0.00723° and 0.00535°, respectively. According to the results of measurements, both samples have as high a crystallinity as that of the other optical grade materials.

For the laser applications, the materials require stable characteristics (transmission), especially around the pumping and the emission wavelengths. As in the case of other complex fluorides [22,23], rather rich induced absorption spectrum of Tm,Ho:LLF (Fig. 9) supports the idea that several kinds of color centers are created under X-ray irradiation. The most frequently induced absorption bands in the UV–visible spectral region in high-quality alkali halides are related to F-centers, i.e. electrons localized in anion vacancies. The position of the F center absorption band is determined by the structure of the material, namely by the distances between the fluorine site and surrounding cations (Molvo–Iwey relation).

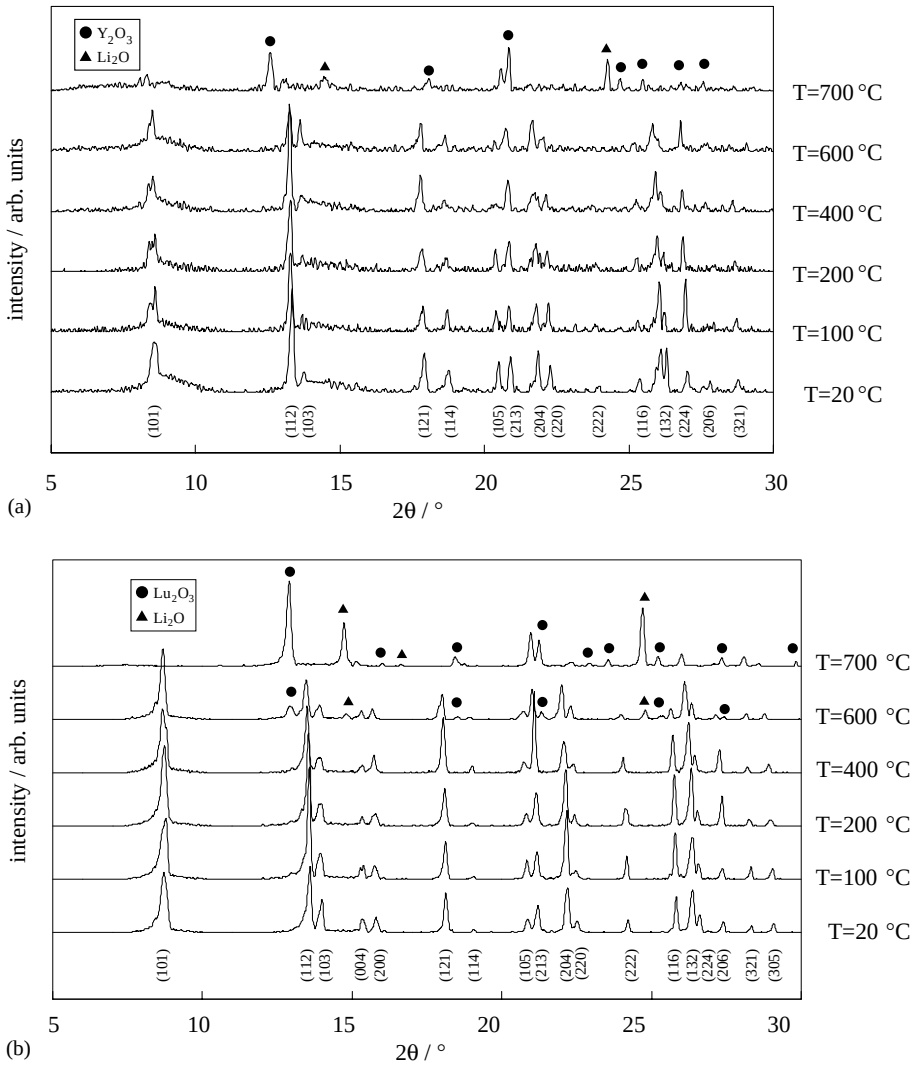

Fig. 5. Dependence of XRD profile on the temperature for (a) 5% Tm and 0.5% Ho-codoped $LiYF_4$ and (b) 5% Tm and 0.5% Ho-codoped $LiLuF_4$ single crystals.

By taking into account the position of the F-center band in LiF (245 nm) and the F–Li distance (2.013 Å), it is reasonable to ascribe the intense absorption band peaking around 315 nm in Tm,Ho:LLF to an F center, since the mean F-to-nearest-cations distance is 2.183 Å. Additional induced absorption bands were produced: they were localized around 240, 380 and 520 nm. The two bands around 240 and 380 nm corresponded probably to perturbed V_k centers, taking into account the several available nearest F–F distances in Tm,Ho:LLF structure (2.549, 2.706, 2.721 Å) and the ascription of 3.99 eV (311 nm) induced absorption band in YLF to V_k-center [24]. The induced absorption band at 520 nm can be most probably related to the F_2 (F_2^+) centers considering its considerably lower amplitude and the long wavelength shift (e.g. in $KMgF_3$, F and F_2 centers are absorbing at 280 nm and 445 nm, respectively [23,25]).

YLF have the same scheelite structure as LLF, with somewhat larger lattice constants (a=5.155 Å (5.150 Å), c = 10.68 Å (10.47 Å) for YLF (LLF)) and similar induced absorption behavior is observed for YLF crystals with respect to LLF. The radiation-induced absorption spectrum after X-ray irradiation for Tm,Ho:YLF is shown in Fig. 9. Similar to Tm,Ho:LLF, no radiation induced absorption bands were found above 700 nm. A three band pattern was found within 200–450 nm similar to Ref. [24]. As with the Tm,Ho:LLF induced absorption, the same bands are observed just shifted toward the longer wavelengths. This is in good accordance with the lattice constant

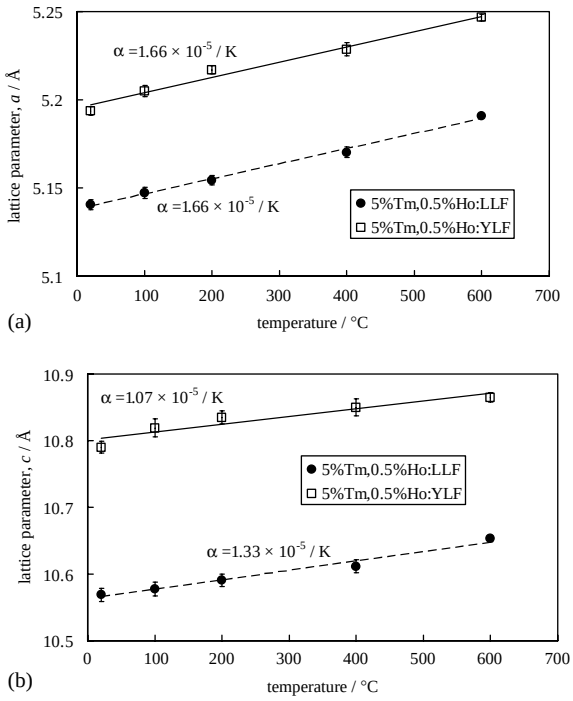

Fig. 6. Dependence of the lattice parameter on the temperature for (a) 5% Tm and 0.5% Ho-codoped $LiYF_4$ and 5% Tm and (b) 0.5% Ho-codoped $LiLuF_4$ single crystals.

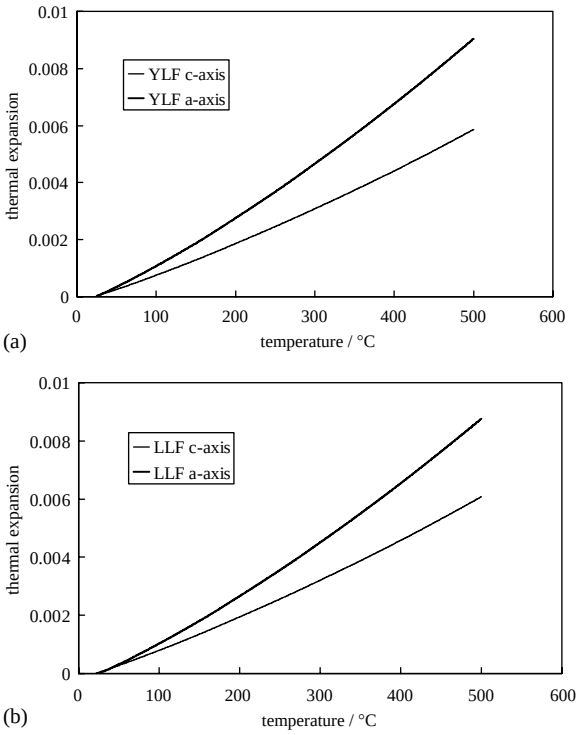

Fig. 7. Dependence of the thermal expansion on the temperature for (a) 5% Tm and 0.5% Ho-codoped $LiYF_4$ and (b) 5% Tm and 0.5% Ho-codoped $LiLuF_4$ single crystals.

Table 1
Linear expansion coefficient and thermal expansion coefficient for Tm,Ho:YLF and Tm,Ho:LLF

	Linear expansion coefficient by XRD measurement (K^{-1})	Thermal expansion coefficient by the thermomechanical analyzing (K^{-1}) at 100°C
5% Tm,0.5% Ho:YLF		
a-axis	1.66×10^{-5}	1.54×10^{-5}
c-axis	1.07×10^{-5}	1.08×10^{-5}
5% Tm,0.5% Ho:LLF		
a-axis	1.66×10^{-5}	1.50×10^{-5}
c-axis	1.33×10^{-5}	1.04×10^{-5}

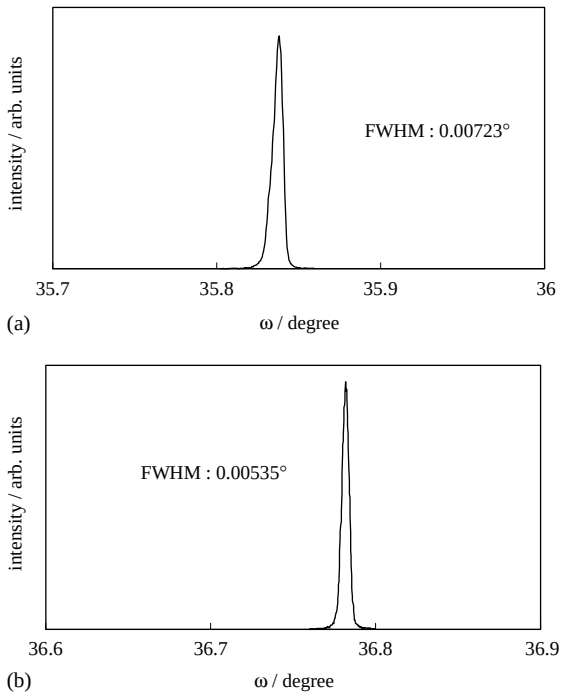

Fig. 8. XRC (ω scan) for (a) 5% Tm and 0.5% Ho-codoped $LiYF_4$ (4 0 0) and (b) 5% Tm and 0.5% Ho-codoped $LiLuF_4$ (0 0 8) single crystals.

relation, i.e. for the same structure, larger lattice constant induces the low energy shift of the bands. F-center band in Tm,Ho:YLF is thus located around 340 nm while it is peaking around 315 nm in Tm,Ho:LLF.

4. Summary

In this work, by modifying the crystal growth conditions, such as the composition of the starting materials and cooling a grown crystal at a position with a lower temperature gradient, Tm,Ho:YLF single crystals 75 mm in diameter (3-in) could be grown. The thermal expansion coefficients of Tm,Ho:YLF (Tm,Ho:LLF) single crystals were calculated to be $1.54 \times 10^{-5}\,K^{-1}$ ($1.50 \times 10^{-5}\,K^{-1}$) along the *a*-axis and $1.08 \times 10^{-5}\,K^{-1}$ ($1.04 \times 10^{-5}\,K^{-1}$) along the *c*-axis. From the XRC measurement, the FWHM values show that the Tm,Ho:YLF and Tm,Ho:LLF crystals have as a high crystallinity as the other optical grade crystals. Induced absorption spectra are governed by the F-center absorption at 315 nm and 340 nm in Tm,Ho:LLF and Tm,Ho:YLF, respectively, and no induced absorption was observed above 700 nm.

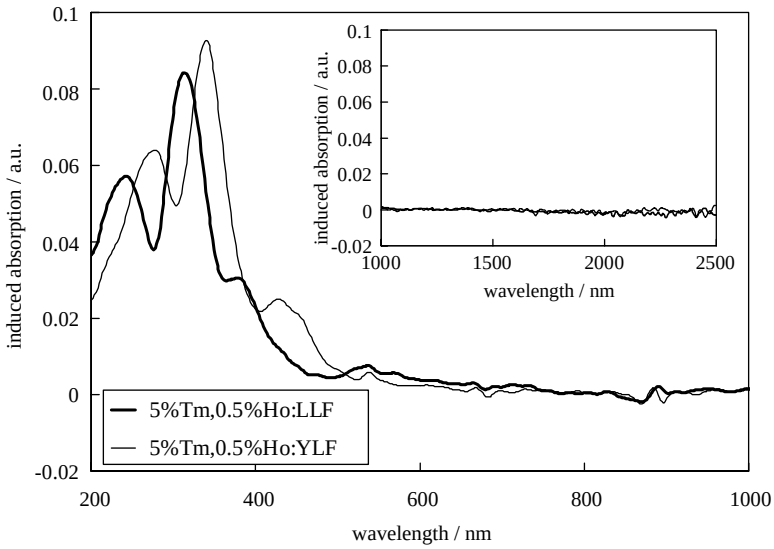

Fig. 9. Induced absorption for (a) 5% Tm and 0.5% Ho-codoped $LiYF_4$ and (b) 5% Tm and 0.5% Ho-codoped $LiLuF_4$ single crystals after X-ray irradiation.

Acknowledgements

The authors would like to thank Mr. Murakami, of the Laboratory for Developmental Research of Advanced Materials in Institute for Materials Research, for his assistance with the X-ray irradiation. This research was performed as part of an R&D program conducted by the Ministry of Economy trade and Industry.

References

[1] V. Sudesh, J.A. Piper, IEEE J. Quantum Electron. 36 (2000) 879.
[2] T. Becker, G. Huber, H.J.V.D. Heide, P. Mitzscherlich, B. Struve, E.W. Duczynski, Opt. Commun. 80 (1) (1990) 47.
[3] R.C. Stoneman, L. Esterowitz, Opt. Photonics News 1 (1990) 10.
[4] V. Sudesh, E.M. Goldys, J. Opt. Soc. Am. B 17 (2000) 1068.
[5] S.A. Payne, L.L. Chase, L.K. Smith, W.L. Kway, W.F. Krupke, IEEE J. Quantum Electron. 28 (1992) 2619.
[6] G. Armagan, A.M. Buoncristiani, B. Di Bartolo, A.T. Inge, C.H. Bair, R.V. Hess, OSA Proc. Tunable Lasers 5 (1989) 222.
[7] T.Y. Fan, G. Huber, R.L. Byer, P. Mitzscherlich, Opt. Lett. 12 (1987) 678.
[8] G.J. Kintz, L. Esterowitz, R. Allen, Electron. Lett. 23 (1987) 616.
[9] T.Y. Fan, G. Huber, R.L. Byer, P. Mitzscherlich, IEEE J. Quantum Electron. 24 (1988) 924.
[10] S.W. Henderson, C.P. Hale, Appl. Opt. 29 (12) (1990) 1716.
[11] H. Sato, K. Shimamura, V. Sudesh, M. Ito, H. Machida, T. Fukuda, J. Crystal Growth 234 (2002) 463.
[12] J. Brenier, J. Rubin, R. Moncorge, C. Pedrini, Proceedings of the International School on Excited States of Transition Elements, Wroclaw, Poland, 1988, World Scientific Pub. Co. PTE Ltd., pp. 14–24.
[13] A. Brenier, J. Rubin, R. Moncorge, C. Pedrini, Crystal J. Phys. 50 (1989) 1463.
[14] L.V.G. Tarelho, L. Gomes, I.M. Ranieri, Phys. Rev. B 56 (22) (1997) 14344.
[15] M. Falconieri, G. Salvetti, Appl. Phys. A 59 (3) (1994) 253.
[16] M.G. Jani, N.P. Barnes, K.E. Murray, D.W. Hart, G.J. Quarles, V.K. Castillo, IEEEE J. Quantum Electron. 33 (1) (1997) 112.
[17] S.L. Baldochi, K. Shimamura, K. Nakano, Na. Mujilatu, T. Fukuda, J. Crystal Growth 205 (1999) 537.
[18] K. Shimamura, S.L. Baldochi, Na. Mujilatu, K. Nakano, Z. Liu, N. Sarukura, T. Fukuda, J. Crystal Growth 211 (2000) 302.
[19] K. Shimamura, Na. Mujilatu, S.L. Baldochi, K. Nakano, Z. Liu, H. Ontake, N. Sarukura, T. Fukuda, J. Crystal Growth 197 (1999) 896.
[20] A. Bensalah, K. Shimamura, V. Sudesh, H. Sato, K. Ito, T. Fukuda, J. Crystal Growth 223 (2001) 539.
[21] F.H. Attix, W.C. Roesch (Eds.), Radiation Dosimetry, Vol. 1, Academic Press, New York, 1968, pp. 112–144 (Chapter 3).
[22] H. Sato, H. Machida, K. Shimamura, A. Bensalah, T. Satonaga, T. Fukuda, E. Mihokova, M. Dusek, M. Nikl, A. Vedda, J. Appl. Phys. 91 (9) (2002) 5666.
[23] H. Sato, K. Shimamura, A. Bensalah, N. Solovieva, A. Beitlerova, A. Vedda, M. Martini, H. Machida, T. Fukuda, M. Nikl, Jpn. J. Appl. Phys. 41 (2002) 2028.
[24] G.M. Renfro, L.E. Halliburton, W.A. Sibley, R.F. Belt, J. Phys. C 13 (1980) 1941.
[25] C.R. Riley, W. Sibley, Phys. Rev. B 1 (1970) 2789.